

A Novel Optimization Algorithm for Buffer and Splitter Minimization in Phase-Skipping Adiabatic Quantum-Flux-Parametron Circuits

Robert S. Aviles, Peter A. Beerel

Department of Electrical and Computer Engineering, University of Southern California, Los Angeles, USA
{rsaviles, pabeerel}@usc.edu

Abstract—Adiabatic Quantum-Flux-Parametron (AQFP) logic is a promising emerging device technology that promises six orders of magnitude lower power than CMOS. However, AQFP is challenged by operation at only ultra-low temperatures, has high latency and area, and requires a complex clocking scheme. In particular, every logic gate, buffer, and splitter must be clocked and each pair of connected clocked gates requires overlapping alternating current (AC) clock signals. In particular, clocked buffers need to be used to balance re-convergent logic paths, a problem that is exacerbated by every multi-node fanout needing a tree of clocked splitters. To reduce circuit area many works have proposed buffer and splitter insertion optimization algorithms and recent works have demonstrated a phase-skipping clocking scheme that reduces latency and area. This paper proposes the first algorithm to optimize buffer and splitter insertion for circuits that adopt phase-skipping and demonstrate the resulting performance improvements for a suite of AQFP benchmark circuits.

I. INTRODUCTION

Computing performance has traditionally enjoyed rapid improvements in energy and area efficiency thanks to the shrinking of transistor sizes following Moore’s law [1] in *complementary metal-oxide-semiconductor* (CMOS) technology. However, after decades of consistent improvements in semiconductor fabrication, transistor sizes are reaching a practical minimum [2] and a performance ceiling for CMOS devices is approaching. This looming end to Moore’s Law, coupled with increasing power densities and a practical limit on clock frequencies for CMOS devices, has driven the demand for emerging device technologies to provide energy-efficient performance improvements. Due to exceptional energy-efficiency, superconductive *single-flux quantum* (SFQ) [3] logic devices have become a promising replacement for CMOS to provide ultra low power consumption in a range of applications from space to exascale supercomputing.

Cooled to 4.2K, Rapid Single Flux Quantum (RSFQ) devices operate at hundreds of GigaHertz with switching energy on the order of 10^{-19} J. However, RSFQ devices require constant DC bias currents which can lead to high static power dissipation. To address this, numerous superconductive designs have been proposed to minimize static power dissipation including efficient rapid single flux quantum (ERSFQ) [4], efficient SFQ (eSFQ) [5], reciprocal quantum logic (RQL) [6], low-voltage RSFQ [7], LR-biased RSFQ [8], and *Adiabatic Quantum Flux Parametron* (AQFP) [9]. AQFP is amongst the most promising of these logic families. Avoiding the inherent static power dissipation issues

associated with DC-biased RSFQ logic types, AQFP utilizes AC-bias currents to consume zero static power [10]. AQFP operates in adiabatic switching at a few GHz and achieves an energy delay product (EDP) at least 200x times smaller than other superconductive logic families and is only three orders of magnitude larger than the quantum limit [9]. Even accounting for the energy overhead to cool to 4.2K, AQFP still achieves two orders of magnitude advantage in EDP compared with state of the art semiconductor technologies [11].

Despite the promising energy-efficiency, AQFP suffers from comparably long latency and poor integration density. Each AQFP logic gate requires an excitation AC clock signal, during which data can propagate from the driving to the receiving gate, which itself requires an active excitation signal to receive the logic signal. Put more simply connected gates require overlapping clock phases to propagate data, forcing connected gates to have adjacent clock phase signals. In large circuits with unbalanced paths this fundamental constraint requires the insertion of buffers to balance re-convergent logic paths, such that buffers can occupy over 90% of the circuit [12]. Further exacerbating this problem, every multi-node fanout needs a tree of clocked splitters, which can lead to further path imbalances. To mitigate these effects and improve circuit integration considerable effort in electronic design automation (EDA) has been made towards minimization of inserted buffer/splitter costs [13]–[17].

In addition, recent works have introduced a notion of phase-skipping via N-Phase clocking [18] and delay-line clocking [19], [20]. These clocking schemes enable overlap between a range of non-adjacent clock phases, allowing driving and receiving gates to have more combinations of respective phases and relaxing strict path balancing constraints. These works promise to dramatically reduce buffer/splitter insertion costs, improving integration density. However, the expanded solution space for valid connections complicates design and all of the existing buffer/splitter optimization algorithms are constrained to adjacent clock phase assignments. To address this issue we propose the first buffer and splitter insertion algorithm to utilize phase-skipping.

- We propose a novel iterative buffer/splitter (B/S) insertion algorithm with polynomial-time runtime that can exploit phase-skipping clocking schemes.
- For circuits that do not support phase-skipping our

polynomial-time solution maintains solution quality across standard benchmarks with an average 0.3% improvement of B/S savings over the state of the art (SOTA) integer linear program (ILP) based method [17].

- For circuits that support phase-skipping, our algorithm shows 48.6%, 63.4%, and 70.3% improvement for 1, 2, and 3 phase-skipping circuits respectively over state of the art circuits without phase-skipping.
- Each iteration of our algorithm includes an optimal level assignment phase-skipping algorithm as an integer linear program (ILP) which we can approximate as an LP to ensure scalability. Moreover, we couple this algorithm with the optimal splitter tree construction presented in [13], [17] modified to support phase-skipping as well as consider allowable extra delay at the fanouts.

II. BACKGROUND

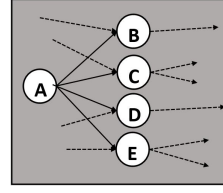
A. AQFP Superconducting Logic

AQFP standard libraries use a minimalist design approach [21] where the very basic gates are majority-3 logic and buffers. All subsequent logic elements can be implemented from modifications to these standard cells and from creating inversions by negating transformer coupling coefficients. AQFP devices store logic states '0' and '1' as a single flux quantum stored in a loop. The internal state is set by the current on the input to the gate and the direction of current on the output is reflective of which internal loop stores the flux quantum. The current input is received while the AC bias current is rising and the output signal is propagated while the bias current is still active. This implies that proper operation requires overlapping clock phases for connected gates [22]. Traditionally, 3-phase and 4-phase clocking has been used where each clock has the same frequency but with a shifted phase. Typically, each gate in a given row is driven by the same clock phase, allowing clock lines to snake throughout the design.

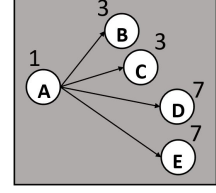
B. Phase-Skipping Clock Schemes

N-Phase clocking has been proposed where a higher number of clock phases is used, with the frequency remaining consistent with 3&4-phase clocking schemes but with smaller phase shifts to accommodate the increased number of phases. As a result, each active clock phase has sufficient overlap with multiple clock phases. For N-Phase clocking a driving gate may directly connect to gates with $\frac{N}{4}$ subsequent phases and maintain the same timing constraints as a 4-phase circuit [18]. This implies that for 8-phase clocking, 1 phase may be skipped. In addition to allowing phase skipping, N-Phase clocking increases the overlap between adjacent clock phases which improves timing margins, and reduces total latency by propagating through more stages of logic per clock cycle.

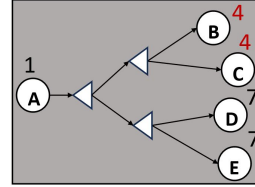
Delay-line clocking [19] uses tuned clock delay lines to shift the clock phase seen by each row of logic, such that overlap appropriate for data synchronization is maintained. Because the latency, or clock skew, between adjacent phases is often much shorter than the phase shift in 4-phase clocking, data can be transmitted across excitation phases [20]. Decreasing



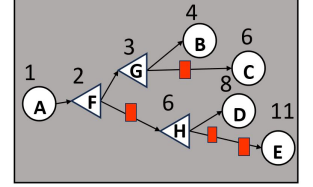
(a) Portion of an initial netlist. Dashed lines indicating connections to other nodes. (Lines omitted for clarity in subsequent images).



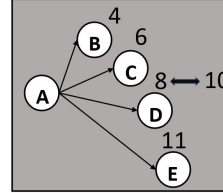
(b) Step 1: Initial level assignments (Section IV-A)



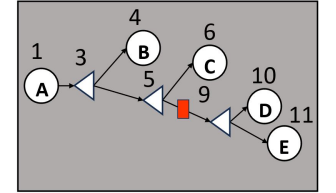
(c) Step 2: Splitter tree insertion (Section IV-B) where levels of B and C were increased to enable splitter insertion.



(d) Step 3: Level assignment for all gates and splitters (Section IV-C).



(e) Step 3b: Removal of all splitters and calculation of slack. (D has an allowable extra delay of 2).



(f) Step 4: Optimal reconstruction of splitter tree. Return to Step 3 and iterate until no improvements are made.

Fig. 1: Example Flow of Proposed Iterative Algorithm

the operating frequency enables larger clock skews to overlap and thus allows for a greater number of phase skips. Using this method up to a phase-skip of 4 in a buffer chain was demonstrated at 3.5 GHz in [20], while for 1 or 2 phase-skipping a frequency of 5.5 GHz was able to be achieved. The EDP of an AQFP gate with delay-line clocking was shown to be $2.8 \times 10^{-32} \text{ J} \cdot \text{s}$, compared to $1.4 \times 10^{-31} \text{ J} \cdot \text{s}$ for 4-phase clocking, and $6.8 \times 10^{-29} \text{ J} \cdot \text{s}$ for RSFQ [20].

Both of these works enable buffer chain reduction of existing circuits, where the existing phase assignments can be utilized to remove buffers that are within the permitted phase-skipping range. However, this only reduces some of the existing buffers and the given gate level assignments are set without exploiting phase-skipping. Our work leverages these phase-skipping schemes to maximally reduce the total buffer and splitter cost of a circuit, achieving 6.7%, 15.6%, and 22.9% savings over buffer chain reduction for circuits with 1, 2, and 3 phase skips respectively.

III. PROPOSED ITERATIVE ALGORITHM OVERVIEW

The main challenge of buffer and splitter insertion in AQFP is that the splitter tree construction affects the degree of imbalance between convergent paths and constrains the optimal

level assignment solution, such that locally optimal splitter trees may not be globally optimal. Similarly, a given level assignment may constrain the available splitter tree configurations.

To address this challenge we first heuristically assign levels while estimating potential splitter tree insertions (Fig. 1b). We then insert locally optimal splitter trees to accommodate the assigned levels, while adjusting levels as needed (Fig. 1c). We then begin our iteration between globally optimal level assignments for a given splitter tree and locally optimal splitter tree construction with given level assignments. Level assignments are conducted for gates and inserted splitters (Fig. 1d). All splitter trees are then removed (Fig. 1e) and an optimal splitter tree is then reconstructed with the new level assignments (Fig. 1f). This iterative cycle continues until no improvements are found between iterations.

Critically, both our level assignments and splitter tree insertion algorithms have polynomial runtimes, allowing multiple iterations to maintain permissible runtimes. After we level assign with splitters inserted, we can guarantee that a valid splitter tree configuration exists without requiring gate re-timing to accommodate subsequent splitter tree insertions. Accordingly, the optimal splitter tree insertion will construct a new splitter tree with lower or the same local cost ensuring that each local splitter tree insertion either improves our global solution or returns a solution of the same quality. Similarly, for a given splitter tree the optimal level assignment step will improve the solution quality or return the same solution.

IV. ITERATIVE ALGORITHM DETAILS

A. Initial Level Assignment

For our iteration start point, before splitter insertion we heuristically provide an initial level assignment. To do this, we model the circuit as a directed acyclic graph (DAG) (V, E) where each gate is an internal node in the graph and circuit inputs (outputs) are input (output) nodes. A directed edge $(E_{ij} \in E)$ is created between each pair of nodes in V that is connected in the circuit. The number of buffers to be inserted between connected nodes i and j is represented as C_{ij} . Each node is assigned a level L_i which directly corresponds to its clock phase assignment. Accordingly, any level difference between connected nodes that exceeds the given circuit's phase skipping constraints requires a buffer insertion. We create constraint (2) to capture the required buffer cost for an allowable overlap of adjacent phases N , such that $N = 2$ for circuits with a phase skip of 1. Following standard design constraints, all primary inputs (PI) are assigned level 0 and all primary outputs (PO) are forced to have equal levels. This leads to the introduction of the following optimization problem:

$$\text{Minimize: } \sum_{E_{ij}=1} \frac{C_{ij}}{|Fanouts_i|} \quad (1)$$

subject to:

$$1 \leq L_j - L_i \leq (C_{ij} + 1) * N \quad \forall (i, j) \in E_{i,j}, \quad (2)$$

$$L_i = L_{outputs} \quad \forall i \in PO, \quad (3)$$

$$L_i = 1 \quad \forall i \in PI, \quad (4)$$

In the Objective Function (Eq. 1) the local costs C_{ij} are divided by the number of fanouts of node i as a heuristic estimate of potential buffer sharing in the splitter tree. To improve our initial solution we add constraints taken from [17] that provide lower bounds on the difference between levels of connected gates, as follows.

$$\sum_{j \in S} (L_j - L_i - 1) \geq f(|S|) \quad \forall i \in v, \forall S \in RS_i \quad (5)$$

These constraints are inspired by the observation that for any subset S of fanout nodes, the *all path sum* of the associated splitter tree must be greater than or equal to that of the minimal all path sum $f(|S|)$ of a complete balanced X -way tree with $|S|$ leaves $B_{|S|}$. Because $B_{|S|}$ is a tree, $f(|S|)$ is equal to the sum of the depths of each leaf of $B_{|S|}$. Put more simply, the levels of any combination S of fanout nodes must leave room for the minimum depth splitter tree that connects the source node to $|S|$ fanouts.

However, for a node with t fanouts, enumerating all possible subsets requires 2^t combinations which becomes prohibitively large. In [17] they fully enumerate trees with up to 30 fanouts which leads to up to 2^{30} (over 1 billion) constraints being added to their ILP for a single splitter tree. Since we are only using constraint (5) for our initial level assignment, we can use a much lower number of constraints K in our formulation. In particular, we set our limit to fully enumerate 15 leaf nodes which corresponds to a maximum of $K = 32,768$ subsets. For nodes with fanouts larger than 15, we randomly generate K subsets. The set of subsets is labelled as RS_i in Eq. 5. Compared to [17], we can employ this more relaxed set of constraints and use an LP instead of an ILP, because the subsequent steps of our algorithm improve upon the initial level assignment resulting from this formulation.

B. Splitter Tree Insertion

We leverage and extend the dynamic-program based optimal splitter tree insertion algorithm presented in [13]. In particular, this algorithm is originally designed for circuits without phase-skipping with the objective to minimize the maximum and total extra delay, where extra delay is the required increase in level assignment for a given node to accommodate splitter tree insertion (Fig. 1c). To assist our iterative algorithm in moving out of local minima, we extend the algorithm to include a notion of allowable slack in extra delay.

In particular, for 2-input gates (Majority-3 gates with a constant input), the allowable extra delay is defined as the difference between the level of the last buffer directly connected to the gate's output in the current solution and the gate's currently assigned level. This extra delay is similar to local retiming slack [23] in that these buffers can be moved across

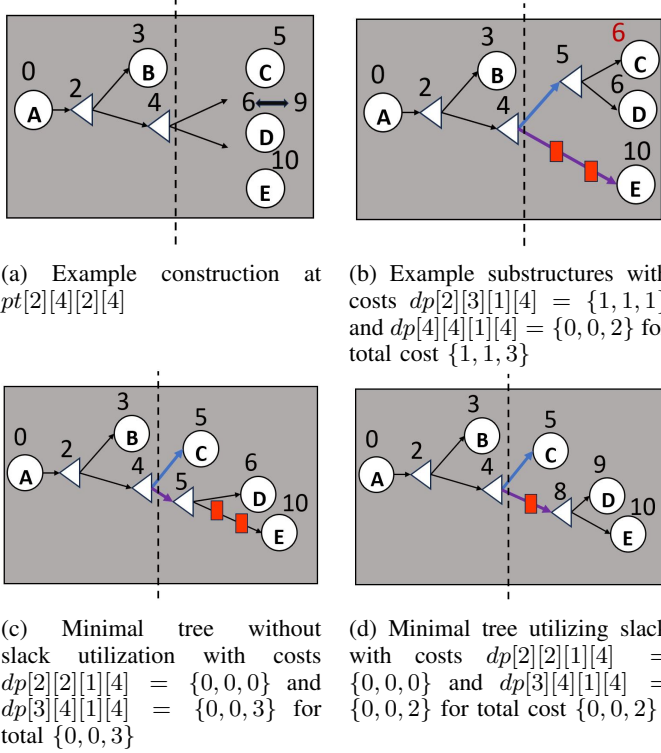


Fig. 2: Example of splitter tree substructure notations at state $pt[2][4][2][4] = \{2, 1, 4\}$

the gate such that the gate can take the level assignment of the last buffer and all constraints would still be met. It is critical that extra delay is only allowed for 2-input gates since retiming a buffer across a gate causes duplicate buffers to be created on each of the gates inputs. However, this extra delay will only occur if it improves the local splitter tree on one of the gates fanin's, in effect absorbing retimed buffers within the local splitter tree.

Our resulting dynamic program is presented in Algorithm 1. We follow the formulation from [17], where $dp_{l,r,b,d}$ records the cost for a tree rooted at level d with b branches that contains leftmost leaf l to rightmost leaf r as $\{maximum\ extra\ delay, total\ extra\ delay, total\ buffer/splitter\ cost\}$, the cost is minimized in descending order of priority where maximum extra delay is given highest precedence. Examples of this notation can be seen in Fig. 2, where 2a shows a partial constructed splitter tree at depth 4 with 2 branches that must contain leafs 2(C) through 4(E). In this example C is assigned delay 5, D is delay 6 with an allowable extra delay of 3, and E has delay 10. Figs 2b - 2d show possible substructures that would have been explored during dp and their respective costs.

The key modifications in our formulation can be found in lines 9,11,18,19, and 23.

- Line 9 allows for a given node to exceed its set level according to its given slack at no cost, but enforces that no node will have extra delay exceeding its slack. An example of the benefit of slack can be seen from comparing the identical splitter tree structures of Fig. 2c and Fig. 2d

where re-assigning to D to delay 9 saves a buffer through increased buffer sharing.

- Line 11, calculates the inserted buffer cost with phase skipping to connect to the given fanout node from level d .
- Line 18, allows for phase skipping within the splitter tree where the optimal solution at a given depth can be built from the minimal cost solution within a span of depths.
- Lines 19 and 23 form the backtracing path in **pt** which records which minimal subtree(s) should be utilized to construct the splitter tree. Our backtracing algorithm differs from those of [13] and [17] as enabling phase-skipping allows the minimal subtree(s) to be constructed from subtree(s) within a range of depths.

Our **pt** or pivot table records an ordered tuple read as $pt[l][r][b][d] = (L_split, branches, depth_next)$. pt indicates which subtree(s) form a minimum cost set of b branches at depth d that contain leaves l through r .

For $b > 1$ the set of branches has been minimally constructed as a disjoint subset of 2 branches. L_split is used to indicate the range of leaves of the left subset as l to L_split and $branches$ now indicates how many of the branches are in the left subset. The right subset takes the remaining leaves and branches such that the 2 next states are $pt[l][L_split][branches][depth_next]$ and $pt[L_split+1][r][b-branches][depth_next]$. As an example, for Fig. 2 the stored result would be $\{2,1,4\}$ indicating that the upper branch contains only the 2nd node (C) and the lower branch should consider the optimal construction of connecting 1 branch from level 4 to the 3rd and 4th nodes. This sets the next state for the second branch as $pt[3][4][1][4]$.

When $b = 1$, the examined set has 1 branch feeding into it and $branches$ indicates how many branches are in the next state. If $branches = 1$ a buffer is to be inserted otherwise a splitter must be inserted to satisfy the increase in fanout. $depth_next$ indicates the next level of the subtree that should be examined such that the next subtree state is $pt[l][r][branches][depth_next]$. The minimal solution from state $pt[3][4][1][4]$ would store $\{-1,1,6\}$ indicating the a buffer is to be inserted at level 6 (Fig. 2d) and to jump to next state $pt[3][4][1][6]$.

By following the pivot table starting at $pt[1][n][1][0]$ the optimal splitter tree can be recovered. Whenever a node is connected to an inserted splitter that has a level assignment greater than or equal to its level plus slack, its level is appropriately adjusted for other local tree insertion steps. For information on the baseline algorithm and proofs of its optimality can be found in the original paper [13].

In total the time complexity of Algorithm 1 is $O(n^3[\log_X n]X^2P_s)$. Where X is a constant set to the maximum fanout of a splitter and P_s is set by the phase overlap of the applied clocking methodology, typically 1 to 4.

C. Optimal Level Assignment

1) *ILP Formulation:* With splitters inserted and treated as nodes, we formulate the clock phase assignment problem of both splitters and gates as an optimization problem minimizing

Algorithm 1: BuildTree(F, X, ps)

Input: F the set of n fanouts of the given source node ordered by ascending delay where $F_i.delay = L(F_i) - L(s) - 1$, X the maximum fanout for a splitter, ps the maximum phase span of connections for the given circuit

Output: pt the pivot table that can construct the optimal splitter tree through backtracking

```
1  $D_{max} \leftarrow F_n.delay + \lceil \log_X n \rceil;$ 
  /* Initialize direct connections */
2 for  $b \in [1, \min\{n, X\}]$ ;  $l \in [1, n - b + 1]$  do
3    $r \leftarrow l + b - 1;$ 
4    $delay \leftarrow F_l.delay;$ 
5   if  $b=1$  then
6     /* Calculate cost to connect to  $l$ 
7       from all depths */
8     for  $d \in [0, D_{max}]$  do
9        $\Delta \leftarrow |d - delay|;$ 
10      if  $\Delta > delay$  then
11         $dp_{l,l,1,d} \leftarrow \Delta >$ 
12         $delay + F_l.slack? \{\Delta, \Delta, 0\} : \{0, 0, 0\};$ 
13      else
14         $dp_{l,l,1,d} \leftarrow \{0, 0, \lfloor \frac{\Delta}{ps} \rfloor\};$ 
15    else
16      /* Calculate cost to connect to  $l$ 
17        through  $r$  from splitter at max
18        level */
19       $dp_{l,r,b,d} \leftarrow dp_{l,r-1,b-1,D_{max}} + dp_{r,r,1,D_{max}};$ 
20  tccBuild minimum cost substructures for
21     $ln \in [1, n - 1]$ ;  $l \in [1, n - ln]$  do
22       $r = l + ln;$ 
23      for  $d = D_{max} - 1$  to 0;  $s \in [1, \min(X, ln + 1)]$  do
24        if  $b = 1$  then
25          /* Find minimum cost
26            substructure connection to
27            buffer or splitter */
28           $dp_{l,r,b,d} \leftarrow$ 
29             $\min_{\substack{\forall k \in [1, \min(X, ln+1)] \\ \forall pr \in [1, \min(ps, D_{max}-d)]}} dp_{l,r,k,d+pr} + 1;$ 
30           $pt_{l,r,b,d} \leftarrow (-1, k, d + pr);$ 
31        else
32          /* Construct set of branches
33            from 2 minimum cost
34            substructures */
35          for  $k \in [1, b - 1]$  do
36             $dp_{l,r,b,d} \leftarrow \min_{p \in [l, r-b+k]} dp_{l,p,k,d} +$ 
37             $dp_{p+1,r,b-k,d};$ 
38             $pt_{l,r,b,d} \leftarrow (p, k, d);$ 
39  return  $pt;$ 
```

the total number of buffers inserted. The constraints are similar to the initial level assignment, however we can directly account for inserted splitters so we no longer require estimates for splitters. Accordingly, Equation 5 is dropped and our objective function (6) directly accounts for all inserted buffers. As such, when integer constraints are enforced (7) we can optimally assign the levels for the given splitter tree and phase-skipping constraints.

$$\text{Minimize: } \sum_{E_{ij}=1} C_{ij} \quad (6)$$

$$L_i, C_{ij} \in \mathbb{N} \quad \forall (i, j) \in E_{i,j} \quad (7)$$

After a solution is returned, the inserted buffer cost plus the number of presently inserted splitters is the total solution cost.

2) *Linear Relaxation:* Considering that the optimal level assignments for a given splitter tree are typically not the final level assignments and the optimal levels will change as the splitter tree configuration adapts, it is worthwhile to relax the integer constraints of the ILP, achieving scalability necessary for successive iterations at a minor sacrifice in solution quality. To handle non-integer values, all returned L_i values are rounded up to the nearest whole number. Since all values are rounded in the same direction, connected nodes that were subject to the relationship $L_j - L_i \geq 1$ before rounding, will still satisfy the constraint after rounding. Some non-optimality is introduced as our objective function may now minimize the sum of fractional buffers (C_{ij}) when $\lceil C_{ij} \rceil$ buffers must be inserted. Importantly, a given iteration may now have a minimal increase in buffer count due to this approximation, in which case the algorithm stops and the previous iterations solution is returned.

V. EXPERIMENTAL RESULTS

All circuit comparisons were made using a common netlist acquired from [24]. In Table I, we compare our benchmark results against the reported state of the art values from [17]. Since runtimes are not reported in [17], we can not make runtime comparisons but our algorithm of polynomial-time complexity achieves results comparable to their reported results without phase-skipping, achieving a minor 0.3% improvement on average. When we exploit phase-skipping clocking schemes our algorithm on average saves 48.6%, 63.4% and 70.3% of total B/S count for circuits with 1,2,and 3 phase-skips enabled.

The only other method to exploit phase-skipping is buffer chain reduction proposed in [18]. In this method an existing netlist is optimized without phase-skipping and inserted buffers that would be redundant under phase-skipping are removed. We apply buffer chain reduction to our 0-phase skipping optimized netlists and compare results to our iterative algorithm for 1, 2 and 3 phase-skipping enabled circuits in Table II. Our results demonstrate the saving benefits of phase-skipping netlist optimization as we achieve 6.7%, 15.6% and 22.9% savings over buffer chain reduction for 1, 2, and 3 phase-skipping circuits respectively.

TABLE I: B/S Savings vs SOTA

Benchmark	Buffer/Splitter Insertion Method				
	SOTA	Our Iterative Algorithm			
	0-Skip	0-Skip	1-Skip	2-Skip	3-Skip
mult8	1681	1674	866	628	539
c432	829	832	429	297	212
c499	1173	1219	665	491	401
c880	1536	1529	745	486	356
c1355	1186	1230	666	485	403
c1908	1253	1253	651	442	359
c2670	1869	1865	892	587	437
c3540	1963	1992	983	686	572
c5315	5505	5510	2708	1803	1386
c6288	8832	8633	4681	3536	3007
Total	25827	25737	13286	9441	7672
Average Savings		0.3%	48.6%	63.4%	70.3%

TABLE II: B/S Savings vs Buffer Chain Reduction

Benchmark	Buffer/Splitter Insertion Method					
	Buffer Reduction			Our Algorithm		
	1-Skip	2-Skip	3-Skip	1-Skip	2-Skip	3-Skip
mult8	941	765	695	866	628	539
c432	419	321	276	429	297	212
c499	702	572	510	665	491	401
c880	798	627	544	745	486	356
c1355	706	580	512	666	485	403
c1908	686	542	476	651	442	359
c2670	954	761	638	892	587	437
c3540	1132	966	882	983	686	572
c5315	2985	2339	2019	2708	1803	1386
c6288	4914	3719	3396	4681	3536	3007
Total	14237	11192	9948	13286	9441	7672
Avg Savings				6.7%	15.6%	22.9%

VI. CONCLUSIONS

As AQFP technology continues to mature, methods to improve circuit integration will need to be improved. To that end we present a tractable algorithm that utilizes phase-skipping in buffer and splitter insertion to achieve 48.6%, 63.4%, and 70.3% for buffer and splitter reduction for 1, 2, and 3 phase-skipping circuits respectively over the state of the art. We hope the strength of these results motivate continued research into phase-skipping implementations and that the presented algorithm assists in the practical implementation of such circuits. Further optimizations can explore applying phase-skipping B/S insertion for sequential circuits, specifically targeting multi-threading. Further power optimizations can be explored such as identifying splitter trees/subtrees where phase-skipping will have minimal impacts and modifying the local constraints to replace phase-skipping splitters with lower-power splitters.

REFERENCES

- [1] G. E. Moore, "Cramming more components onto integrated circuits, reprinted from electronics, volume 38, number 8, april 19, 1965, pp.114 ff." *IEEE Solid-State Circuits Society Newsletter*, vol. 11, no. 3, pp. 33–35, 2006.
- [2] T. N. Theis and H.-S. P. Wong, "The end of moore's law: A new beginning for information technology," *Computing in Science & Engineering*, vol. 19, no. 2, pp. 41–50, 2017.
- [3] K. Likharev and V. Semenov, "RSFQ logic/memory family: a new josephson-junction technology for sub-terahertz-clock-frequency digital systems," *IEEE TASC*, vol. 1, no. 1, pp. 3–28, 1991.
- [4] D. E. Kirichenko, S. Sarwana, and A. F. Kirichenko, "Zero static power dissipation biasing of rsfq circuits," *IEEE TASC*, vol. 21, no. 3, pp. 776–779, 2011.
- [5] O. A. Mukhanov, "Energy-efficient single flux quantum technology," *IEEE TASC*, vol. 21, no. 3, pp. 760–769, 2011.
- [6] Q. P. Herr, A. Y. Herr, O. T. Oberg, and A. G. Ioannidis, "Ultra-low-power superconductor logic," *Journal of Applied Physics*, vol. 109, no. 10, May 2011. [Online]. Available: <http://dx.doi.org/10.1063/1.3585849>
- [7] M. Tanaka, M. Ito, A. Kitayama, T. Kouketsu, and A. Fujimaki, "18-ghz, 4.0-aj/bit operation of ultra-low-energy rapid single-flux-quantum shift registers," *Japanese Journal of Applied Physics*, vol. 51, no. 5R, p. 053102, may 2012. [Online]. Available: <https://dx.doi.org/10.1143/JJAP.51.053102>
- [8] N. Yoshikawa and Y. Kato, "Reduction of power consumption of rsfq circuits by inductance-load biasing," *Superconductor Science and Technology*, vol. 12, no. 11, p. 918, nov 1999. [Online]. Available: <https://dx.doi.org/10.1088/0953-2048/12/11/367>
- [9] N. Takeuchi, D. Ozawa, Y. Yamanashi, and N. Yoshikawa, "An adiabatic quantum flux parametron as an ultra-low-power logic device," *Superconductor Science and Technology*, vol. 26, no. 3, p. 035010, jan 2013. [Online]. Available: <https://dx.doi.org/10.1088/0953-2048/26/3/035010>
- [10] Y. Okuma, N. Takeuchi, Y. Yamanashi, and N. Yoshikawa, "Miniaturization of adiabatic quantum-flux-parametron circuits by adopting offset buffers," *Superconductor Science and Technology*, vol. 32, no. 6, p. 065007, may 2019. [Online]. Available: <https://dx.doi.org/10.1088/1361-6668/ab1672>
- [11] O. Chen, R. Cai, Y. Wang, F. Ke, T. Yamae, R. Saito, N. Takeuchi, and N. Yoshikawa, "Adiabatic quantum-flux-parametron: Towards building extremely energy-efficient circuits and systems," *Scientific reports*, vol. 9, no. 1, p. 10514, 2019.
- [12] C. L. Ayala, R. Saito, T. Tanaka, O. Chen, N. Takeuchi, Y. He, and N. Yoshikawa, "A semi-custom design methodology and environment for implementing superconductor adiabatic quantum-flux-parametron microprocessors," *Superconductor Science and Technology*, vol. 33, no. 5, p. 054006, mar 2020. [Online]. Available: <https://dx.doi.org/10.1088/1361-6668/ab7ec3>
- [13] C.-Y. Huang, Y.-C. Chang, M.-J. Tsai, and T.-Y. Ho, "An optimal algorithm for splitter and buffer insertion in adiabatic quantum-flux-parametron circuits," in *2021 IEEE (ICCAD)*, 2021, pp. 1–8.
- [14] R. Cai, O. Chen, A. Ren, N. Liu, N. Yoshikawa, and Y. Wang, "A buffer and splitter insertion framework for adiabatic quantum-flux-parametron superconducting circuits," in *2019 IEEE (ICCD)*, 2019, pp. 429–436.
- [15] A. T. Calvino and G. De Micheli, "Depth-optimal buffer and splitter insertion and optimization in aqfp circuits," in *2023 28th ASP-DAC*, 2023, pp. 152–158.
- [16] S.-Y. Lee, H. Riener, and G. De Micheli, "Beyond local optimality of buffer and splitter insertion for aqfp circuits," in *59th Design Automation Conference*, ser. DAC '22. New York, NY, USA: Association for Computing Machinery, 2022, p. 445–450. [Online]. Available: <https://doi.org/10.1145/3489517.3530661>
- [17] R. Fu, M. Wang, Y. Kan, N. Yoshikawa, T.-Y. Ho, and O. Chen, "A global optimization algorithm for buffer and splitter insertion in adiabatic quantum-flux-parametron circuits," in *2023 28th ASP-DAC*, 2023, pp. 769–774.
- [18] R. Saito, C. L. Ayala, and N. Yoshikawa, "Buffer reduction via n-phase clocking in adiabatic quantum-flux-parametron benchmark circuits," *IEEE Transactions on Applied Superconductivity*, vol. 31, no. 6, pp. 1–8, 2021.
- [19] N. Takeuchi, M. Nozoe, Y. He, and N. Yoshikawa, "Low-latency adiabatic superconductor logic using delay-line clocking," *Applied Physics Letters*, vol. 115, no. 7, p. 072601, 08 2019. [Online]. Available: <https://doi.org/10.1063/1.5111599>

- [20] T. Yamae, N. Takeuchi, and N. Yoshikawa, "Adiabatic quantum-flux-parametron with delay-line clocking: logic gate demonstration and phase skipping operation," *Superconductor Science and Technology*, vol. 34, no. 12, p. 125002, Oct. 2021. [Online]. Available: <http://dx.doi.org/10.1088/1361-6668/ac2e9f>
- [21] N. Takeuchi, Y. Yamanashi, and N. Yoshikawa, "Adiabatic quantum-flux-parametron cell library adopting minimalist design," *Journal of Applied Physics*, vol. 117, no. 17, p. 173912, 05 2015. [Online]. Available: <https://doi.org/10.1063/1.4919838>
- [22] N. Takeuchi, S. Nagasawa, F. China, T. Ando, M. Hidaka, Y. Yamanashi, and N. Yoshikawa, "Adiabatic quantum-flux-parametron cell library designed using a 10 ka cm^2 niobium fabrication process," *Superconductor Science and Technology*, vol. 30, no. 3, p. 035002, jan 2017. [Online]. Available: <https://dx.doi.org/10.1088/1361-6668/aa52f3>
- [23] C. E. Leiserson and J. B. Saxe, "Retiming synchronous circuitry," *Algorithmica*, vol. 6, no. 1-6, pp. 5–35, 1991.
- [24] EPFL, "Isacas'85 and simple arithmetic benchmarks." 2021. [Online]. Available: <https://github.com/lisil/SCE-benchmarks>